Atmospheric Research 176–177 (2016) 108–120

Contents lists available at ScienceDirect

Atmospheric Research

journal homepage: www.elsevier.com/locate/atmosres

$PM_{2.5}$ chemical composition at a rural background site in Central Europe, including correlation and air mass back trajectory analysis

Jaroslav Schwarz [a,*], Michael Cusack [a], Jindřich Karban [a], Eva Chalupníčková [b], Vladimír Havránek [c], Jiří Smolík [a], Vladimír Ždímal [a]

[a] Institute of Chemical Process Fundamentals, CAS, Prague, CZ-16502, Czech Republic
[b] Czech Hydrometeorological Institute, Prague, CZ-14306, Czech Republic
[c] Nuclear Physics Institute, Řež at Prague, Czech Republic

ARTICLE INFO

Article history:
Received 13 October 2015
Received in revised form 16 February 2016
Accepted 17 February 2016
Available online 24 February 2016

Keywords:
Rural aerosol
PM2.5
Chemical composition
Correlation analysis
Air mass back trajectory

ABSTRACT

$PM_{2.5}$ mass concentrations and chemical compositions sampled over a 13-month period at a Central European rural background site (Košetice) are presented in this work. A comprehensive chemical analysis of $PM_{2.5}$ was performed, which provided elemental composition (Al, Si, S, Cl, K, Ca, Ti, V, Cr, Mn, Fe, Ni, Cu, Zn, As, Se, Br, Rb, Sr, Y, Zr, and Pb) and the concentration of water-soluble inorganic anions (SO_4^{2-}, NO_3^-, Cl^-, NO_2^-, Br^-, and $H_2PO_4^-$) and cations (Na^+, NH_4^+, K^+, Ca^{2+}, and Mg^{2+}), elemental and organic carbon (EC and OC), and levoglucosan. Spearman correlation coefficients between individual chemical species and particle number concentrations were calculated for the following six size ranges: 10–25 nm (N10–25), 25–50 nm (N25–50), 50–80 nm (N50–80), 80–150 nm (N80–150), 150–300 nm (N150–300), and 300–800 nm (N300–800).

Average concentrations of individual species were comparable with concentrations reported from similar sites across Central Europe. Organic matter (OM) accounted for 45% of the $PM_{2.5}$ mass (calculated from OC by a factor of 1.6), while the second most common component were secondary aerosols (SO_4^{2-}: 19%, NO_3^-: 14%, NH_4^+: 10%), which accounted for 43% of the mass. Based on levoglucosan analysis, 31% of OM was attributed to emissions associated with biomass burning (OM_{BB}). EC concentrations, determined using the EUSAAR_2 thermal optical protocol, contributed 4% to $PM_{2.5}$ mass. A total of 1% of the mass was attributed to a mineral matter source, while the remaining 6% was from an undetermined mass. Seasonal variations showed highest concentrations of NO_3^- and OM_{BB} in winter, nitrate share in spring, and an increase in percentage of SO_4^{2-} and mineral matter in summer. The largest seasonal variation was found for species associated with wood and coal combustion (levoglucosan, K^+, Zn, Pb, As), which had clear maxima during winter. Correlation analysis of different size fraction particle number concentrations was used to distinguish the influence of fresh, local aerosol and aged, long-range transport aerosol.

The influences of different air masses were also investigated. The lowest concentrations of $PM_{2.5}$ were recorded under the influence of marine air masses from the NW, which were also marked by increased concentrations of marine aerosol. In contrast, the highest concentrations of $PM_{2.5}$ and most major chemical components were measured during periods when continental easterly air masses were dominant.

1. Introduction

Atmospheric aerosols have been of environmental concern since the Industrial Revolution. The discovery and increased understanding of their detrimental health and environmental effects gave rise to policies and directives aimed at controlling levels of pollutants in the atmosphere through, for example, control of ambient concentrations of PM_{10} and $PM_{2.5}$.

Measurements at rural background sites are important, as they are beyond the influence of urban emissions and are, therefore, better suited for investigating the influence of long-range transport and long-term trends in concentrations, both of which are essential to climate change studies. Obligatory measurement of PM_{10} within the E.U. has been in place for the last decade, resulting in an increased understanding of chemical concentrations and compositions around across Europe. A comprehensive summary of these measurements was performed by Putaud et al. (2004), but data from post-communist countries were omitted due to a lack of long-term data.

Nevertheless, some older studies on PM and chemical composition in Central Europe do exist. PM_2 levels and elemental composition were measured at Bílý Kříž, a rural site in the Northeastern Czech Republic, by Swietlicki and Krejci (1996), while Borbely-Kiss et al. (1999) studied urban and rural sites in Hungary. Horvath et al. (1996) described PM (sampled by impactors) for the urban area of Vienna and its surroundings, and two studies were performed by Maenhaut

* Corresponding author at: Rozvojová 135, 16502 Prague 6 - Suchdol, Czech Republic.
E-mail address: schwarz@icpf.cas.cz (J. Schwarz).

http://dx.doi.org/10.1016/j.atmosres.2016.02.017
0169-8095/

et al. (2005, 2008) on the fine and coarse fractions in Budapest and $PM_{2.5}$ and PM_{10} at K-Puzsta.

The recent implementation of a 25 μg m^{-3} $PM_{2.5}$ limit in the EU led to an increase in measurement campaigns across Europe, including post-communist countries. Even with this data available, which included measurements from over 60 stations across Europe, a 2010 follow-up of Putaud et al.'s work only included $PM_{2.5}$ data from four sites among post-communist countries (Prague, Debrecen, and two rural Hungarian sites). Although Košetice, the site of this study, is also mentioned in the 2010 study, only PM_{10} mass and TC were reported.

During the sampling for this study, several other studies on $PM_{2.5}$ at rural background sites in Central Europe were performed, and their published results are as follows. Spindler et al. (2013) described the long-term trends of PM_{10} (20 years) and $PM_{2.5}$ and PM_1 (10 years) for the rural background site of Melpitz in Germany. From 1993 to 2000, a decrease in PM_{10} was found, and from 2000 to 2011, no discernible trend was observed for any PM fraction. During the period of overlap between our work at the Košetice site and this study, the average $PM_{2.5}$ values were roughly 17–19 μg m^{-3}.

Rogula-Kozłowska et al. (2014) reported $PM_{2.5}$ concentrations of 15 μg m^{-3} for the Diabla Gora rural background station in northern Poland. $PM_{2.5}$ concentrations at a rural site near Vienna were 18.1 μg m^{-3} (Puxbaum et al., 2004) and Hueglin et al. (2005) measured $PM_{2.5}$ concentrations of 7.7 μg m^{-3} for a high-altitude site in Switzerland (Chaumont; 1000 m a.s.l.). Both of these studies took place near the end of the period with decreasing $PM_{2.5}$ values (Spindler et al., 2013) and, therefore, may have been influenced by the not yet fully implemented emission controls in the former communist Eastern European countries.

Recently published results on continuous measurements of $PM_{2.5}$ chemical composition for rural regions of the Czech Republic, or long-term analysis of $PM_{2.5}$ (longer than one year) in Europe, are currently scarce. Moreover, studies performed in Central Europe before 2000 were strongly influenced by poor cleaning of industrial sources and the use of leaded petrol in passenger cars. A recent increase in the use of wood combustion for residential heating has also changed emission profiles, which might have a direct influence on emission levels and chemical composition of $PM_{2.5}$. Consequently, the aim of this study is to fill in these gaps by providing further information regarding $PM_{2.5}$ composition and concentration from a Central European rural background site.

2. Experimental

2.1. Sampling site

All samples were collected at the Košetice rural background site (N49°35′, E15°05′; 534 m a.s.l.). The site is classified as representative of the regional background in the Czech Republic. The Košetice site is located 60 km SE of the urban area of Prague, and the closest medium-sized urban area lies 15 km to the south, with a population of 16,000. There are also several small settlements within a 3 km radius, of which Košetice village is the largest, at 3 km to the SE and a population of 700. The village of Kramolin is the closest settlement, and is 1.2 km away to the SW with only around 10 permanent inhabitants. One of the major national highways is situated 6 km north of the site, with two more settlements of 1000 inhabitants within the same distance. Finally, a small wood factory equipped with a biomass furnace (about 10 years old) lies 7.5 km from the site. The Košetice measurement station is part of the EMEP, ACTRIS (formerly EUSAAR), and GAW networks.

2.2. Sampling

$PM_{2.5}$ was sampled for 24 h on every sixth day from February 5, 2009 to April 1, 2010 using Leckel and Derenda low-volume samplers equipped with $PM_{2.5}$ sampling inlets. The flow rate was set to 2.3 m^3/h at both samplers, and was controlled using built-in mass flowmeters. The distance between the two samplers was 2.5 m. Two $PM_{2.5}$ samples were collected in parallel by one sampler loaded with TEFLO filters (Pall, 47 mm in diameter, 2 μm pore size) and another loaded with two pre-baked (3 h, 800 °C) quartz fibre filters (Tissuequartz, Pall, 47 mm) placed in series (face to face). The front quartz fibre filter was downstream of the inlet and collected aerosol particles, while the back filter, placed downstream of the front filter, only collected absorbable organic vapours. In total, there were 71 sampling days when $PM_{2.5}$ samples were collected on both TEFLO and quartz fibre filters.

All filters were weighed before and after sampling with 1-μg resolution Sartorius M5P micro balances in a designated weighing room with climate control (RH: 30%–40%; temperature: 20 °C–25 °C). In order to assess the impact of unstable conditions, control filters were regularly weighed during each weighing run and their weight changes were used to correct measurements of the other filters. Field blanks were collected regularly from both samplers, during which time filters were placed in the samplers and exposed to 10 s of sampling. This resulted in 10 field blanks for the Teflon filters and 14 field blanks for the quartz fibre filters. These filters were then analysed using the same method as the sample filters, and all data were corrected according to the blank filters. No statistically significant difference was found between the front and back quartz fibre filter blanks, so these results were averaged and used for blank corrections on both front and back quartz fibre filters. The field blanks were analysed the same way as filters with samples and all data were corrected using the blank values.

The filters were stored in Petrislides (Millipore) and kept in closed double polyethylene ZIP bags. The filters were stored at room temperature prior to sampling, whereas after sampling the filters were stored in a fridge (4 °C) prior to weighing and analysis.

2.3. Chemical analysis

2.3.1. Ion chromatography

Circular punches measuring 19 mm were cut out from each quartz fibre filter and were subsequently water-extracted for 30 min with 5 mL of ultra-pure water (<0.2 μS.cm^{-1}; Ultrapure, Watrex, Czech Republic) in an ultrasonic bath, followed by a 1 h treatment in a mechanical shaker. The resulting suspension was filtered using a 25 mm syringe filter with 0.22 μm porosity. The filtered sample was then analysed for anions (SO_4^{2-}, NO_3^-. Cl^-, NO_2^-, Br^-, $H_2PO_4^-$) and cations (Na^+, NH_4^+, K^+, Ca^{2+}, Mg^{2+}, Zn^{2+}). The analysis was performed using the apparatus setup by Watrex Ltd., with a Transgenomic ICSep AN300 150 × 5.5 mm column for anions (using eluent and analytical conditions aligned with the column application sheet at http://www.chromtech.com/products/hplc_columns/ion/transgenomic/transgenomic_ionanalysis.pdf). An Alltech universal cation 7 μm 100 × 4.6 mm column was used for cations (using eluent and analytical conditions aligned with the column application sheet at http://www.obrnutafaza.hr/pdf/grace/Alltech/IC/Alltech-IC-Applications-Cations.pdf). A SHODEX CD-5 conductive detector was used. The external calibration was performed at the beginning and end of each analysis batch using six-level calibration solutions with NIST traceable standard stock solutions. The average between the two calibrations was used as the calibration curve.

2.3.2. OC/EC analysis

A 1.5 cm^2 punch of each filter was analysed using the EUSAAR 2 temperature program, as described in Cavalli et al. (2010). All $PM_{2.5}$ quartz fibre filters (both front and back filters of the pair of quartz fibre filters sampled in series in one $PM_{2.5}$ sampler) were analysed for OC and EC using the thermal optical transmission (TOT) method (Birch and Cary, 1996) in a Sunset Laboratory Thermal–Optical Aerosol Analyzer at the Czech Hydrometeorological Institute.

The OC concentrations measured from the front and back filters are referred to as OC1 and OC2, respectively. The difference between OC1 and OC2 was taken as the measured ambient particulate OC

concentration (OC = OC1 − OC2). Thus, the OC values reported throughout this manuscript have been corrected for positive absorption artefacts. Total carbon (TC) was calculated as the sum of OC and EC.

2.3.3. PIXE

The $PM_{2.5}$ samples collected on TEFLO filters were analysed for elemental composition by PIXE analysis using a 3.5 MV Van de Graff accelerator in the Nuclear Physics Institute in Řež, Czech Republic. All 71 samples were analysed using a proton beam of 2.2 MeV, beam diameter of 5 mm, and beam current of about 10 nA. The proton energy was used to optimize the signal to background ratio for medium and high Z elements with respect to the high gamma background from this particular Teflon filter. Measurements typically ranged from 800 to 1000 s, resulting in an average collected charge of 10 μC per analysis. A specially designed chamber for simultaneous measurement by PIXE, PIGE RBS, and PESA techniques was used (Havránek et al., 2004). In this particular case, only PIXE spectra from two Si(Li) detectors were used. Up to Ca, the elements were detected by the low Z detector, which had a 30 mm^2 active area and a 170 eV resolution (at Mn Kα line) without an X-ray absorption filter. The elements above Ti were detected using an 80 mm^2 (180 eV resolution) detector and a 0.8-mm-thick PE X-ray absorption filter. The proton dose (collected charge normalization) was determined using a specially designed, thin Ni foil (0.5 μm) RBS monitor. Generally, the concentrations of the 22 elements (Al, Si, S, Cl, K, Ca, Ti, V, Cr, Mn, Fe, Ni, Cu, Zn, As, Se, Br, Rb, Sr, Y, Zr, and Pb) were determined from the filters; however, only concentrations of 12 elements (Al, Si, S, Cl, K, Ca, Ti, Mn, Fe, Cu, Zn, and Pb) were above the detection limits on most of the filters. A set of thin MICROMATTER™ filters were used to calibrate the PIXE and the PIXE-INP computer code (Havránek et al., 1994), which was used to determine the elemental surface mass densities of aerosol deposits (in $\mu g/cm^2$). Additionally, ten (field) blank filters were analysed, and the blank corrections were subtracted and the blank concentration variances were introduced into the expanded uncertainty of obtained concentrations. The blank filters were almost free of contamination—significant values were only found for Al, Si, and Fe. However, the blank variance factors were also added into the S, Ca, Cl, K, Ca, Br, and Pb uncertainty values. Finally, the air mass concentrations were calculated using a known effective deposit area of 12 cm^2 and normalized air volume collected the filters. The total relative uncertainty budget of PIXE analysis can be estimated as follows: 5% relative uncertainty for efficiency calibration, 2% for charge normalization, 5% for conversion from mass density to air volume concentration, and 1%–30% for peak area fitting (depends on the counting statistic of particular peak).

2.3.4. Levoglucosan (LVG) analysis

The analytical method described by Zdráhal et al. (2002) was employed and is briefly outlined here. A solution of 1,2,3-trihydroxyhexane in methanol (c = 10.0 mg/25 mL) was prepared and used as an internal standard. A 19 mm diameter piece was cut out from each filter and was spiked with 1,2,3-trihydroxyhexane (4 μg). These were placed in a sonic bath, along with 10 mL of a dichloromethane–methanol solvent mixture (4:1), for 15 min. The extracts were filtered and concentrated under reduced pressure (ca 400 mbar) to about 1 mL, then transferred to 2 mL vials and evaporated under a stream of nitrogen until dry. A trimethylsilylation mixture (50 μL, *N*-methyl-*N*-trimethylsilyltrifluoroacetamide containing 1% trimethylchlorosilane-pyridine 2:1) was added and the vials were kept at 70 °C for 1 h to complete trimethylsilylation. The analysis was carried out using an Agilent HP 6890 gas chromatograph coupled with an HP 5973 mass selective detector. The silylated sample (1 μL) was injected into a split/splitless injector operating in the split mode 1:10 at 250 °C. The oven was set at 100 °C and held for 3 min, then programmed to 220 °C at a rate 10 °C/min, and then to 290 °C at 30 °C/min. The final temperature (290 °C) was held for 10 min. Helium was used as a carrier gas and was at a flow-rate of 1 mL/min. A DB-5 ms capillary column (30 m × 0.25 mm × 0.25 μm) was used for separation. The mass spectrometer operated in 70 eV ionization mode, the ion source temperature was set at 230 °C, and acquisition was done in the scan mode, with the range 35–400 m/z. The fragment ion m/z 204 was used for quantification of LVG, and m/z 217, 73, and 333 were used as confirmation ions. The fragment ions m/z 145 were used for quantitation and m/z 73 for confirmation of trihydroxyhexane. Linear calibration curves ($R^2 > 0.998$) were obtained in the range 0.04–20 μg/mL using five gravimetrically prepared solutions of LVG. A laboratory blank, via an unexposed filter, was included in every eight samples and processed in the same way as field samples. No levoglucosan was detected in laboratory blanks.

2.4. Calculation of $PM_{2.5}$ species

Organic matter (OM) was calculated from OC by multiplying by a factor of 1.6 (Turpin and Lim, 2001), which accounts for hydrogen, oxygen, and other elements present in ambient organic aerosol. However, this value may be considered very conservative for a rural background site, as higher values have recently been suggested by, for example, El-Zanan et al. (2005). Poulain et al. (2011) found a ratio of 1.65–1.8 (night–day) in summer and 1.6–1.67 in winter for Melpitz. Therefore, the calculated OM may be viewed as the lower limit of the real OM concentration.

OM mass was then split into two fractions: biomass burning OM (OM_{BB}) and non-biomass burning OM (OM_{REST}). OM_{BB} was derived from OC_{BB} by multiplying by 1.6. This factor was chosen based on H:C and O:C ratios for combustion of spruce wood (Elsasser et al., 2013) and the probable subsequent oxidation of primary OM_{BB} during transport, which takes into account the rural background location of the site. OC_{BB} was calculated from the measured LVG concentrations by multiplying LVG concentration by a factor of 10 as described by Szidat et al. (2009). This factor was based on independent OC_{BB} determination and LVG analysis in ambient samples. Therefore, it includes, in contrast to the data from emission measurements, not only primary OC_{BB} but also secondary OC_{BB}, which direct emission measurements cannot account for. In addition to those connected with determining a suitable concentration factor, other uncertainties exist when calculating OM_{BB} from LVG concentrations. For example, LVG is prone to atmospheric oxidation, which leads to an atmospheric lifetime on the order of days (Lai et al., 2014). Additionally, non-negligible concentrations of LVG have been found in emissions from young lignite combustion in Poland (Fabbri et al., 2009). Even though this type of lignite is rarely used for residential heating in the Czech Republic Machálek and Machart (2003), emissions may still influence the OM_{BB} concentrations reported in this work.

Crustal material, further referred to as "soil," was determined by calculating concentrations of oxides from concentrations of crustal elements (Al_2O_3, SiO_2, CaO, TiO_2, MnO_2, and Fe_2O_3) using the following oxide factors: Al (1.890), Si (2.139), Ca (1.400), Ti (1.668), Mn (1.582), and Fe (1.430).

The concentrations of sea salt ions (Na^+, Mg^{2+}, Cl^-), potassium (K), and trace elements (Cu, Zn, As, and Pb) were so low that they were combined for mass closure analysis and are referred to as "elements" in that chapter.

2.5. Number size distribution data

The aerosol particle number size distributions were measured continuously with 5-min time resolution in parallel with filter sampling (10 to 800 nm). A SMPS (IFT Tropos, Leipzig, with CPC 3022 (TSI, USA)) was run according to EUSAAR SOP (Wiedensohler et al., 2012), and average 24-h concentrations were calculated for six size fractions (10–25 nm (N10–25), 25–50 nm (N25–50), 50–80 nm (N50–80), 80–150 nm (N80–150), 150–300 nm (N150–300), and 300–800 nm (N300–800)). More details about these measurements, including QA/QC procedures, can be found in Zíková and Ždímal (2013).

2.6. Calculations

2.6.1. Spearman correlations

Due to an insufficient number of sampling days, positive matrix factorization analysis could not be performed successfully. Therefore, correlation analysis was performed in order to identify possible interactions between the species. A correlation matrix of Spearman correlation coefficients (r) was calculated using R statistical software when all data was available (55 sampling days, including the 24-h average particle number concentrations in the above mentioned size bins). Moreover, Spearman correlations for the heating season (October 16–April 15, 35 sampling days) and non-heating season (April 16–October 15; 20 sampling days), defined in agreement with Schwarz et al. (2008), were calculated separately.

2.6.2. Back trajectory calculation

The 96-h air mass back trajectories (AMBT) were calculated using HYSPLIT (Draxler and Rolph, 2013; Rolph, 2013) four times for each 24-h sample and at three different heights (100, 500, and 1500 m AGL). The sampling days were split into four categories based on the daily prevailing AMBT. First were days with easterly continental origins (Econt, Fig. S1), when the majority of the trajectories were from areas east of Prague, excluding Finland and the other Nordic countries. Second were the north–west air masses (NW), which were mostly connected to sea-influenced air masses from the Atlantic. Third were south–west air masses (SW, from southern France to Italy), which were sometimes connected to Saharan dust events. Finally, fourth were the western continental air masses (Wcont), which were connected to westerly air masses, but only those that mainly existed over land. The number of cases in each category were as follows: Econt (23, HS-13, NHS-10), NW (20, HS-13, NHS-7), SW (10, HS-7, NHS-3), and Wcont (18, HS-7, NHS-11).

2.7. QA/QC procedures

All data presented here were field blank corrected, which constituted about 10% of the analysed filters. The field blank values for water-soluble ions were generally low, and only nitrates ($0.006 \pm 0.006\ \mu g\ m^{-3}$), sulphates ($0.005 \pm 0.003\ \mu g\ m^{-3}$), sodium ($0.010 \pm 0.003\ \mu g\ m^{-3}$), and ammonium ($0.005 \pm 0.003\ \mu g\ m^{-3}$) existed at detectable concentrations. With the exception of sodium, the blank values had almost no influence on the water-soluble ion data. Ion chromatography filter extraction efficiencies were checked using the repeated extraction of samples that had already been extracted for standard analysis. The results of the repeated analysis never exceeded 5% of the value obtained during the first analysis of any given sample for sulphates, nitrates, or ammonium.

The IC uncertainty was determined by repeating the analysis of a sample 10 times and by evaluating the differences between the first and second calibrations. In both cases, the power law equation was obtained by fitting it into error dependence on the concentration level.

The errors caused by operations not included in these experiments were added using the error propagation law. Generally, the errors caused by analysis were under 5% for solutions with concentrations above 1 ppm, while they increased rapidly to 20%–40% for concentrations around 0.1 ppm, and even more if the analysed concentration was lower. (Similar results were also found when triplicates from the same filter were analysEd.)

Occasionally, the front quartz fibre filter in the series was exposed to water, resulting in contamination of the back filter by water-soluble components that had been originally captured on the front filter. In order to correct for this contamination, we assumed that the water-soluble species on the back filter were originally deposited on the front filter. Furthermore, under dry circumstances sulphate concentrations on the back filter were very low (near the field blank values). Therefore, when concentrations of sulphate on the back filter ($SO_4^{2-}{}_B$) exceeded 5% of the front filter concentrations ($SO_4^{2-}{}_F$), the influence of water leakage was assumed and a correction was applied based on the equation used for OC. For example:

$OC_{corr} = OC1 + OC2 - 2^{*}OC2_{av}$, where $OC2_{av}$ is the average concentration of OC on the back filters (excluding those where $SO_4^{2-}{}_b/SO_4^{2-}{}_f > 0.05$).

The 5% threshold was used, as a smaller value would not have caused a change larger than the measurement uncertainty and was also high enough to separate from changes caused by blank uncertainty or possible small contamination during sample manipulation. This was also done for other species, and the resulting corrected concentrations were compared with data provided by PIXE analysis, which weren't affected by the same problem. This correction was applied to around 15% of all samples.

As both Teflon and quartz fibre filters were weighted, we compared the $PM_{2.5}$ mass from quartz fibre filters ($PM_{2.5Q}$) to the Teflon filters. The average $PM_{2.5Q}/PM_{2.5}$ ratio was 1.13 ± 0.22 after the correction for water leakage was applied. The Teflon filter mass data was treated as final, as quartz filters may gain or lose mass when they are face to face.

In general, we believe that the high quality of the employed analytical procedure is reflected in the mass closure study, which lead to the determination of 90% of total mass, on average, with water contributing to the remaining $PM_{2.5}$ mass.

3. Results and discussions

3.1. Average composition

Average concentrations of all measured components of $PM_{2.5}$ are presented in Table 1, along with the median, standard deviations of the mean, and seasonal average concentrations. Differences in average and median concentrations for total $PM_{2.5}$ and many analysed species indicate that concentrations were not normally distributed, as they were influenced by periods of stable and stagnant atmospheres with high $PM_{2.5}$ concentrations.

There are two pairs of components with similar qualities in the table; K and K^+ and S and SO_4^{2-}. K^+ (analysed by Ion Chromatography) is water-soluble, whereas elemental K, as measured by PIXE, may have also included insoluble K (e.g. from mineral dust). When these differences are taken into account, it can be assumed that the majority of the K in $PM_{2.5}$ existed in the water-soluble K^+ form. Further similarities were found between S and SO_4^{2} concentrations if S concentrations were used to recalculate SO_4^{2} concentrations. Again, this allowed for the assumption that the majority of S existed as SO_4^{2}. Accordingly, this paper uses the PIXE elemental K values and ion chromatography sulphate values.

The average $PM_{2.5}$ concentration ($15.7\ \mu g\ m^{-3}$) at Košetice was close to the values found at other rural sites in Central Europe (Spindler et al., 2013; Rogula-Kozłowska et al., 2014; Puxbaum et al., 2004), suggesting relatively homogenous background concentrations in Central Europe. A much smaller average $PM_{2.5}$ concentration of $7.7\ \mu g\ m^{-3}$ was found by Hueglin et al. (2005) at a higher altitude site in Switzerland (Chaumont; 1000 m a.s.l.). The differences in source strength and meteorological patterns connected with higher altitude were probably the reasons for the lower concentration.

Carbonaceous aerosols (TC) were the largest component of $PM_{2.5}$ at the Košetice site (31% based on average of seasonal averages of individual sample shares), which is significantly more than the 17% average reported by Putaud et al. (2010) for rural Central European sites. Nonetheless, TC concentrations at Košetice fall within the range of other rural background sites around Europe. TC concentrations at Melpitz ($3.5\ \mu g\ m^{-3}$) and Diabla Gora ($3.7\ \mu g\ m^{-3}$) were somewhat lower than those measured at Košetice ($4.69\ \mu g\ m^{-3}$). In terms of seasonal changes, Pio et al. (2007) reported summer and winter TC concentrations of 8 and 13 $\mu g\ m^{-3}$, respectively, at the K-Puszta station in

Table 1
Average (total and seasonal), median, and standard deviation of $PM_{2.5}$, and its measured chemical components (in μg m^{-3}), and number concentration in six size fractions.

	Average	Median	St. Dev	Spring	Summer	Autumn	Winter
μg m^{-3}							
$PM_{2.5}$	15.7	11.8	9.4	14.0	9.7	16.5	22.5
EC	0.61	0.51	0.34	0.63	0.36	0.64	0.80
OC	4.07	3.00	2.66	3.93	2.12	4.09	6.00
TC	4.69	3.35	2.92	4.56	2.48	4.73	6.80
Na^+	0.037	0.027	0.031	0.041	0.030	0.035	0.039
NH_4^+	1.52	1.24	1.03	1.58	0.96	1.53	1.92
K^+	0.092	0.059	0.077	0.079	0.034	0.100	0.151
Mg^{2+}	0.004	0.003	0.005	0.006	0.003	0.003	0.003
Cl^-	0.04	0.02	0.04	0.04	0.01	0.04	0.05
NO_3^-	2.20	1.73	2.34	2.53	0.55	2.52	2.83
SO_4^{2-}	2.85	2.22	2.05	2.51	2.30	2.78	3.86
LVG	0.125	0.089	0.111	0.097	0.020	0.130	0.237
ng m^{-3}							
Al	30.2	22.6	37.0	24.6	30.5	34.4	34.1
Si	59.6	38.9	86.3	58.8	79.5	68.3	39.8
S	1102	818	802	898	842	1171	1544
K	108.1	76.7	85.5	81.8	40.3	129.7	181.5
Ca	12.3	9.8	13.3	14.6	15.0	13.4	6.8
Ti	2.12	1.46	2.58	2.07	2.58	2.52	1.60
Mn	1.46	1.24	1.25	1.16	1.26	1.70	1.83
Fe	28.8	22.0	27.2	26.4	31.3	37.8	23.6
Cu	0.89	0.77	0.63	0.77	0.73	1.12	1.00
Zn	15.2	10.3	11.8	14.4	6.1	16.4	23.0
As	0.75	0.25	0.74	0.58	0.43	0.73	1.19
Pb	4.94	3.62	4.48	5.05	2.67	4.26	7.36
#/cm^3							
10–25	1567	1225	1326	1874	2327	1357	974
25–50	1438	1201	1122	1641	1878	1264	1119
50–80	984	922	442	984	1077	962	967
80–150	1207	1213	555	1090	1153	1256	1365
150–300	913	850	412	857	825	858	1101
300–800	275	211	186	244	173	267	384

Hungary, which are much higher than levels measured at Košetice (summer and winter values of 2.48 and 6.80 μg m^{-3}, respectively). This difference may have been due to K-Puszta's larger neighbouring populations, lower dilution of emissions, lower altitude (and, therefore, lower mixing), higher photochemical interaction in summer, and higher influence of biomass burning (see LVG concentration comparison below).

Quantitative comparisons with similar sites show that sulphate concentrations at Košetice are slightly higher than those reported at Melpitz (about 2.5 μg m^{-3}) or Diabla Gora (2.6 μg m^{-3}), but nitrate concentrations are lower than at Melpitz (3.4 μg m^{-3}) and at Diabla Gora (2.1 μg m^{-3}). Sulphate concentrations at K-Puszta in summer (4 μg m^{-3}) and winter (5 μg m^{-3}) are higher than at Košetice (2.3 and 3.86 μg m^{-3}, respectively). Nitrate concentrations in summer time (0.5 μg m^{-3}) at K-Puszta were similar to summer concentrations at Košetice (0.55 μg m^{-3}), but winter concentrations (6 μg m^{-3}) were much higher. Similar reasons to those mentioned above for TC may be responsible for this difference.

Concentrations of Ca (0.11 %), Na^+, Mg, K, and Cl^- were lower than those reported for the sites mentioned above. Na^+(0.34%), Cl^- (0.23%), and Mg(0.03%) concentrations, which are primarily associated with marine aerosol, are typically low for this region of Europe. Putaud et al. (2010) showed that marine aerosol represented around 1% of $PM_{2.5}$ for rural sites in this region of Europe, which is in line with concentrations for Košetice. Cl^- may have had other sources, such as combustion, and existed as ammonium chloride where thermodynamically feasible. Levels of Mg were also low at this site, and may also have been related to low levels of Mg found in Czech calcite (Hartman et al., 2003). Fine fraction K (0.66%) is often considered a typical tracer for biomass burning (Schauer et al., 1996; Caseiro et al., 2009), which is a significant source of aerosols in Central Europe. Similar concentrations of K^+ (0.09 μg m^{-3}) were reported for Diabla Gora (0.11 μg m^{-3}) and the range of rural sites surrounding Paris (0.10–0.12 μg m^{-3}; Bressi et al., 2013). However, a marine source of K was probably more influential at these sites than at Košetice.

Descriptions of levels of trace elements for this region of Europe are uncommon, especially over a similar time period as this work. Although the percentage of trace elements in $PM_{2.5}$ is generally low (Ti 0.017%, Mn 0.011%, Fe 0.21%, Cu 0.010%, Zn 0.093%, As 0.006%, Pb 0.029%), they may have important consequences on aerosol-related health effects (Duvall et al., 2008) or aerosol chemistry (Berglund et al., 1993). Levels of As at Diabla Gora were lower than those reported here (0.20 ng m^{-3} and 0.61 ng m^{-3} for the HS and NHS, respectively), but Pb levels were higher. Puxbaum et al. (2004) reported levels of various elements composing $PM_{2.5}$ at a rural site in Austria from 1999 to 2000. Arsenic (0.66 ng m^{-3}) and Mn (2.0 ng m^{-3}) levels were about 30% higher than Košetice, Fe (23 ng m^{-3}) and Zn (17 ng m^{-3}) levels were similar to the concentrations found at Košetice, and concentrations of Cu (1.7 ng m^{-3}) were two times higher. Pb levels (12 ng m^{-3}) were 2.5 times higher than at Košetice, but this was probably related to the use of leaded petrol in the neighbouring post-communist countries at that time.

Finally, levels of LVG at Košetice (0.13 μg m^{-3}, 0.74% in $PM_{2.5}$) were intermediate; levels at the K-Puszta rural site in Hungary (0.31 μg m^{-3}; 136 m a.s.l., Puxbaum et al., 2007) were significantly higher, while concentrations in the rural mountain site of Schauinsland (Germany, 1205 m a.s.l.) were lower (0.02 μg m^{-3}). The authors believe the variations in concentrations were besides the different source strength within the areas also due to altitude and mixing layer heights in winter.

Average concentrations of size segregated particles exhibit seasonal dependance. Its nature is related to particle size.

The smallest size fractions exhibited maximum concentrations in summer, while the largest particles had maxima in winter. This trend is consistent among size fractions, with the change of maximum in

number concentration from summer to winter at 80 nm; i.e. all three smaller fractions have maximum in summer and all three larger fractions have maximum in winter. More detailed characterisations of particle number size distribution at the Košetice site can be found in Zíková and Ždímal (2013).

3.2. Seasonal variability

The ratios of average seasonal concentrations to the annual average concentrations for all analysed chemical species are depicted in Fig. 1. As is evidenced in Fig. 1, the highest seasonal variability was found for LVG—a specific marker of biomass combustion (Simoneit et al., 1999).

The large difference between summer and winter LVG concentrations was probably caused mainly by wood combustion for domestic heating. Furthermore, LVG has a shorter atmospheric lifetime during summer as a result of photochemical activity, higher temperatures, and lower RH relative to winter (Lai et al., 2014). Puxbaum et al. (2007) showed an even higher seasonal difference for LVG at the K-Puszta site. The concentration with the second-highest seasonal variation was potassium, which is mainly produced via wood combustion during winter (Fine et al., 2001). Similar variations within Zn concentrations might also suggest wood combustion as a source for this $PM_{2.5}$ (Sippula et al., 2009); however, incinerators, metallurgy, and coal combustion are also sources of Zn (Pacyna and Pacyna, 2001). Lead and arsenic also show similar seasonal variations, and are produced by, in addition to industrial sources, coal combustion from domestic heating in the Czech Republic and other post-communist countries (Machálek and Machart, 2003). Organic and total carbon also exhibit similar seasonal distributions, as they are the major components of PM; this variation is likely related to winter sources of wood and coal combustion.

The high seasonal variability of nitrates, with their maximum concentrations in winter, is related to the thermal instability of ammonium nitrate (Seinfeld and Pandis, 1998), which leads to lower concentrations during the daytime and may also result in losses of nitrates captured on the filter (Zhang and McMurry, 1992). The large difference between chloride in summer and all other seasons may be related to several factors working together (Fig. 1). First, there is, on average, lower sea salt influence during summer in Central Europe. This is due to meteorological factors in the Northern Atlantic and North Sea (where the majority of the sea salt comes from; Siegismund and Schrum, 2001); these areas are also connected with fast air mass transport to Central Europe. Second, the volatility (or dissociation) of ammonium chloride in summer (Harrison et al., 1990) is similar to that of ammonium nitrate, which leads to lowered concentrations. Third, both biomass and coal combustion sources of chloride are much lower and there is an absence of road salt in summer.

Nevertheless, there is no winter maximum of Na^+ at the Košetice site, suggesting that road salt was not a dominant factor impacting $PM_{2.5}$ Na^+ concentration levels. All the remaining species that had maximum winter concentrations had a lower seasonal variability relative to their total mass. Sulphates exhibited a maximum in winter, but otherwise had relatively stable concentrations throughout the year. EC had additional combustion sources in the form of residential heating (Watson et al., 2001; Schmidl et al., 2011) during colder months, but its main source, traffic, was constant throughout the year. Gelencsér et al. (2007) found a more than 10-fold increase of EC from biomass burning at K-Puszta, while there was only a 10% increase in EC from fossil fuels, suggesting that biomass burning had a larger influence on EC levels than coal during winter months. Even so, differences can be expected between Hungary and Czech Republic due to the different fuel mixes used for residential heating. Mn remained constant throughout the year, indicating it had a stable, consistent, and probably industrial source.

Cu, Fe, and Al had the highest average seasonal concentrations in autumn. It is difficult to ascertain the cause, as they are not associated with common sources (although Cu and Fe may come from break debris, and Al and Fe from mineral dust) and have different seasonality profiles. It is likely that a combination of different sources occurred, coincidentally explaining this behaviour. Finally, the remaining elements (Ti, Si, and Ca) are typical crustal elements. Their summer maxima was likely related to soil resuspension, which is inhibited in winter due to snow cover and high humidity. Saharan dust intrusions, while uncommon for this region of Europe, may also have had limited influence.

3.3. PM chemical components

The comprehensive chemical analysis of $PM_{2.5}$ allowed for a detailed mass balance to be performed. The seasonal and yearly mass closure was performed by recalculating the concentrations of measured species to their probable chemical compound or class.

Secondary inorganic ions (SIA), which are formed mainly by ammonium sulphate and ammonium nitrate, comprised 43% of the $PM_{2.5}$ mass. This was in line with results summarised by Rogula-Kozłowska et al. (2014), which were somewhat higher than the SIA percentage found in Diabla Gora (36%), and similar to or lower than SIA percentages of $PM_{2.5}$ at three French rural sites (42%, 48%, 48%; Bressi et al., 2013).

Sulphates represented 19% of the $PM_{2.5}$ mass, which was similar to the average of 17% share of sulphates at rural Central European sites in Putaud et al. (2010). Bressi et al. (2013) found somewhat lower percentages (15%, 16%, and 16%) of sulphate at his three rural French sites.

Nitrates exhibited a 13% share of $PM_{2.5}$; this was similar to the more than 10% share of nitrate in $PM_{2.5}$ in three of the four Central European

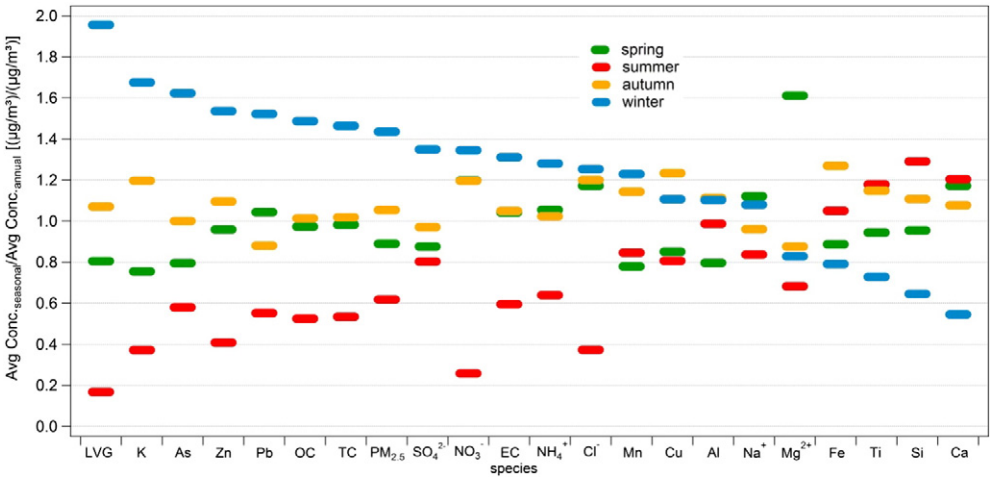

Fig. 1. The ratios of average seasonal concentrations relative to the average of all seasons for all analysed chemical species.

rural background sites in the study by Putaud et al. (2010), but much lower than the 17%, 22%, and 21% shares of nitrate found by Bressi et al. (2013). The higher share of nitrates than sulphates in $PM_{2.5}$ in France suggests lower SO_2 sources than the Czech Republic and/or higher ammonia concentrations, which allow for higher ammonium nitrate formation.

Elemental carbon represented 4% of the $PM_{2.5}$ mass. As EC determination is method-dependent (Chow et al., 2001), direct comparison can only be done between works using the same thermo-optical method and analytical protocol. Bressi et al. (2013) found the same percentage of EC (4%) at all three rural sites using the same thermal-optical method and analytical protocol. A higher percentage of EC was found for urban sites in their work (9% at suburban and 10% at urban sites), which can be expected by the influence of traffic. An EC share in $PM_{2.5}$ up to 10% was also reported for urban sites in southern Europe by Salameh et al. (2015). "Soil" represents only 1% of $PM_{2.5}$, which indicated the small influence of crustal aerosol at Košetice site. It was lower than other sites; Rogula-Kozlowska found an 8% share of crustal material in $PM_{2.5}$ at their three sites and Hueglin et al. (2005) shows share of crustal material in the range of a few percent at Swiss sites.

"Elements" also formed 1% of $PM_{2.5}$ altogether; when they are split into three subgroups, K itself represent 0.5%, which supports the relatively high influence of biomass burning (especially if we take into account the small influence of other K sources—mineral dust and sea salt). This was followed by sea salt-like ions (Na^+, Mg^{2+}, Cl^-), with 0.3%, and trace elements (Cu, Zn, As, and Pb), representing 0.1% of $PM_{2.5}$.

The difference between the analytically assigned mass and gravimetrically determined mass (called "rest" in Fig. 2) may have resulted from undetected species (e.g. water) and/or the difference between the applied and real OM/OC ratio. This may have also partially explained the relatively high share of "rest" in summer (Fig. 3 c), as higher oxidation occurs during periods of higher photochemical activity. This was observed by Poulain et al. (2011) in Melpitz, where the aerosol mass spectrometer measured a higher PM_1 organic aerosol (OA, equivalent to OM) to OC ratio (1.73) in summer than in winter (1.64).

The seasonal mass closures shown in Fig. 3 reveal a relatively low variation in the share of carbonaceous aerosols among seasons. The combined share of OM and EC varies from 44% in summer to 53% in winter. There was much higher variability at the Diabla Gora site (Rogula-Kozłowska et al., 2014), where the minimum share of carbonaceous aerosol was 19% in spring and a maximum of 44% in winter.

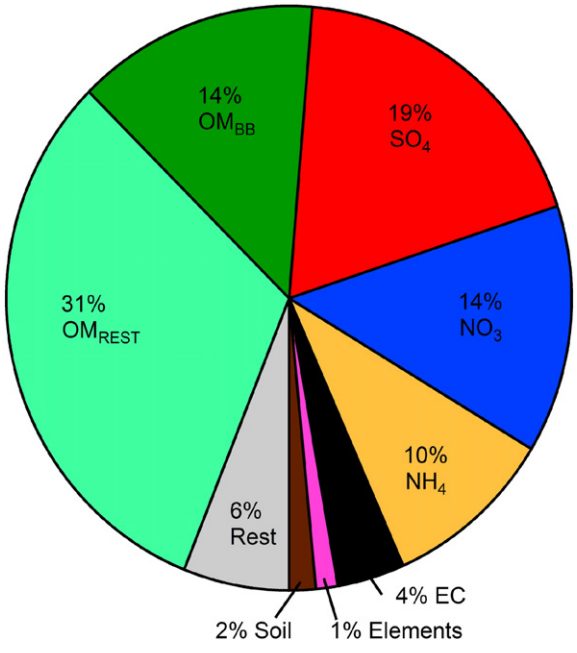

Fig. 2. Annual average composition of $PM_{2.5}$ at the Košetice site.

The OM share in $PM_{2.5}$ varies from 40% in summer to 49% in winter. This low variability suggests a higher relative importance of combustion sources in winter than SOA formation in summer. Similar seasonal variation was found in Barcelona and Marseille by Salameh et al. (2015), who found a minimum OM share in the summer and a maximum in the winter.

As is to be expected in Central Europe, especially when considering the LVG seasonal variation described above, the highest seasonal change in a $PM_{2.5}$ component share was for OM_{BB}, whose share increased from 4% in summer to 19% in winter. Furthermore, OM_{BB} constituted 10% of the total OM per sample in summer, but increased to 48% in winter. This agrees reasonably well with data reported from K-Puszta (Gelencsér et al., 2007), where OC_{BB} constitutes 6% of TC in summer and 40% in winter. On the other hand, the Košetice cold period values are lower than those from Ispra, where 53% of the TC was OC_{BB} (Gilardoni et al., 2011), or the Münich/Augsburg area, where 51.6% OC was OC_{BB} (Jedynska et al., 2015). Although the contribution to $PM_{2.5}$ was lower (12%), our winter OM_{BB} percentage of $PM_{2.5}$ was much smaller than in Oslo (28.3%, Jedynska et al., 2015). The high winter influence of biomass burning at the Košetice site may have been due to the use of old stoves and wood burning for residential heating in nearby villages.

OM_{REST}, which represents an organic mass from sources other than biomass burning, exhibited a weak cycle that was opposite to that of OM_{BB} and OM in regards to its share in $PM_{2.5}$; its minimum share was in winter (30%) and maximum in summer (36%). Coal combustion (Machálek and Machart, 2003), traffic, and industry are probably the major sources of OM_{REST} in winter, while secondary organic aerosol, traffic, and industry are probably the major sources in summer.

In each season, the elemental carbon EC represented 4% of the $PM_{2.5}$, which was probably caused by the unchanging nature of its major source—traffic. Furthermore, this is connected, both directly and indirectly, with Central European combustion processes

Inorganic secondary ion (SIA, sulphates, nitrates, and ammonium) shares in $PM_{2.5}$ vary from 40% in summer and winter to 47% in spring, showing similar, or slightly lower, importance of SIA in $PM_{2.5}$ relative to carbonaceous species at Košetice. This is in line with Bressi et al. (2013), where a roughly similar percentage can be seen for SIA and carbonaceous aerosols in $PM_{2.5}$.

Sulphate itself represented between 17% in autumn and 24% of $PM_{2.5}$ in summer. The higher percentage in summer than other seasons may be, at least partially, attributed to reduced nitrates in $PM_{2.5}$ mass and faster SO_2 photochemical oxidation in summer (Seinfeld and Pandis, 1998), and possibly some influence of biochemical production of sulphur organic compounds in marine environments (Uher et al., 2000).

Nitrates exhibited a minimum $PM_{2.5}$ share of 5% in summer and maximum of 18% in spring, which is a much higher seasonal dependence than exhibited by sulphates. The spring maximum might have been caused by higher availability of ammonia in spring (Horváth and Sutton, 1998; Kopáček et al., 1997) when temperatures are still favourable for ammonium nitrate formation (Seinfeld and Pandis, 1998). Although the ammonia emission can be higher in summer, the high temperatures during this season do not allow for ammonium nitrate formation during the day. At the same time, sulphate concentrations are lower in spring than in winter, the amount of ammonia needed for sulphate neutralization is lower, and more ammonia is available for ammonium nitrate formation. However, this behaviour differs from the Polish Diabla Gora rural site, where the highest seasonal share of nitrates in $PM_{2.5}$ was observed in winter (Rogula-Kozłowska et al., 2014).

"Soil" showed maximum average seasonal concentrations in summer (3% of $PM_{2.5}$). Crustal elements may have different origin—road dust resuspension (Lough et al., 2005, Limbeck et al., 2009), field work resuspension (both of which may be increased due to low average RH (70%) in summer), long-range transport of Saharan dust (Schwikowski et al., 1995), or Ukrainian dust which was also observed (Birmili et al., 2008;

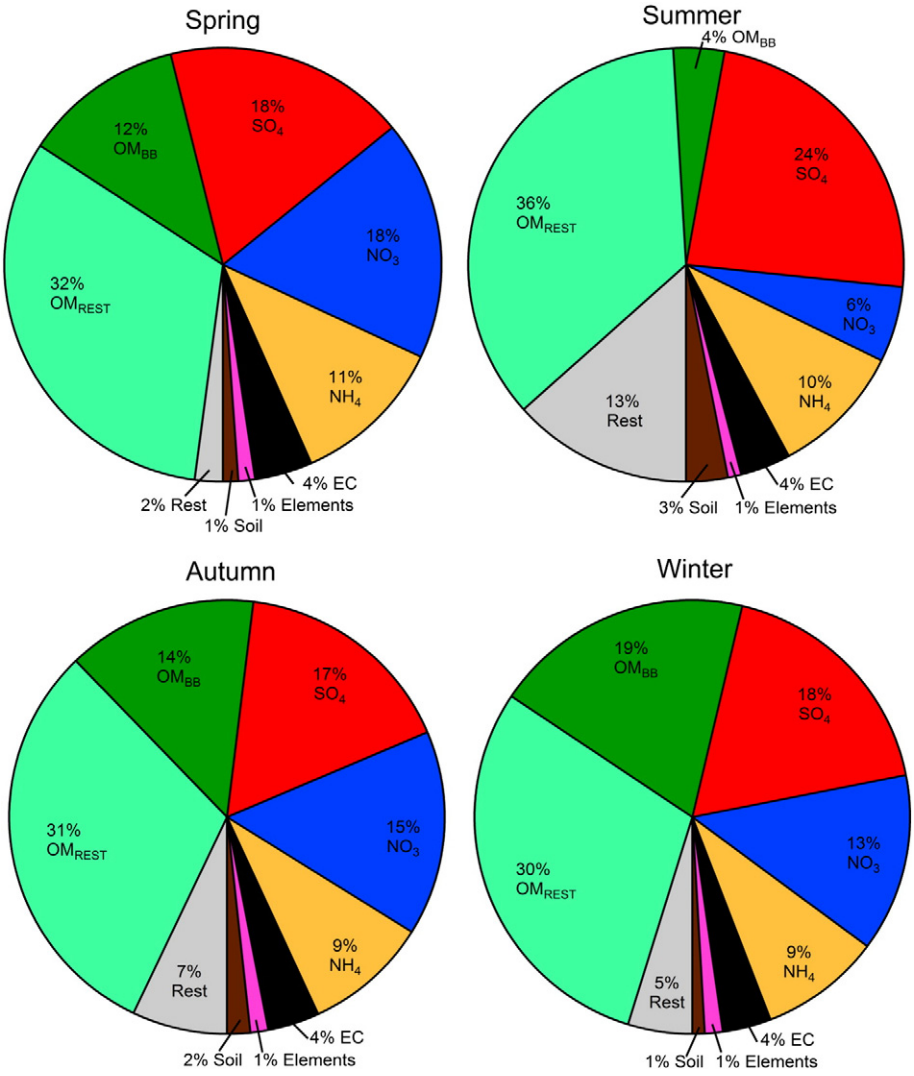

Fig. 3. Seasonal average $PM_{2.5}$ chemical composition at the Košetice site.

Hladil et al., 2008), and finally some of these elements may also have industrial, traffic (Fe) or building (Ca) sources. A fraction of crustal elements in $PM_{2.5}$ may also be influenced by combustion sources. Moreover, the influence of long-range transport and combustion sources may increase in $PM_{2.5}$ in comparison with PM_{10} or $PM_{2.5-10}$ fractions as smaller fractions of long-range transported dust have smaller deposition rates in comparison with coarse particles. The minimum soil share was found in winter (1%) when snow cover may prevent resuspension and RH is often high (86% on average).

The "elements" had a constant share (1%) of the $PM_{2.5}$ throughout the year. However, when split into their subgroups, K exhibited a maximum share of 0.6% in winter and a minimum of 0.3% in summer, which, again, supports a wood combustion influence in winter. Sea salt-like ions had maximum percentage in spring (0.4%) and minimum in winter (0.2%), while trace elements had a constant share of 0.1%, with a slightly higher share in spring.

3.4. Correlations of species

For the whole sampling period (Table S1), the influence of secondary inorganic ions on $PM_{2.5}$ mass is confirmed by high correlation of $PM_{2.5}$ with ammonium (Spearman correlation coefficient $r = 0.90$) and sulphate (0.81), and moderate correlation with nitrate (0.62).

The influence of carbonaceous aerosol on $PM_{2.5}$ was reflected in the $PM_{2.5}$ correlation coefficient with OC (0.82) and EC (0.73). A relationship between $PM_{2.5}$ and industrial sources connected with metal production can be inferred from its high correlation with Zn (0.89) and Pb (0.78) (Pacyna et al., 2007). A high correlation of $PM_{2.5}$ with K (0.84) suggests the important influence of biomass burning. A high correlation between $PM_{2.5}$ with number concentration of particles of mobility diameters between 300 and 800 nm (N300–800) was found (0.90). Such a high correlation coefficient with particles of this size suggests the importance of aged and cloud processed aerosol at this site. A similar relationship of aged particles with particles larger than 300 nm was shown by Gu et al. (2011), Cusack et al. (2013), and Beddows et al. (2015). A lower, but still high, correlation was found for N150–300 (0.75), suggesting the influence of more local sources.

Sulphates, as a part of secondary inorganic aerosol, were correlated with ammonium (0.88), as expected, but also with Pb (0.74) and Zn (0.69), suggesting industrial and coal combustion origins. Correlations with particle number size fractions N300–800 (0.72) confirmed the influence of aged and cloud processed aerosols at the site and moderate correlation was still found for N150–300 (0.60).

During the entire period, nitrate was correlated with ammonium (0.71), LVG (0.65), Zn (0.58), and N300–800 (0.62). Although the nitrate correlation with N300–800 was lower than the correlation of this size fraction with sulphates, the much smaller correlation of nitrate with smaller particles than that of sulphates supports relatively high influence of aged particles.

Carbonaceous aerosol is related with combustion emissions, especially biomass burning. This seems true for OC (high correlation coefficient with EC (0.79), K (0.82), Zn (0.82) and LVG (0.71)), and for EC (high correlation coefficients for K (0.84), Zn (0.83), and LVG (0.77)). Correlations with particle number size fractions were more evenly distributed among three size categories (OC: N300–800 (0.75), N150–300 (0.68), N80–150 (0.62); EC: N300–800 (0.65), N150–300 (0.59), N80–150 (0.52)), suggesting a mixture of both aged and more fresh carbonaceous aerosol origins. Attribution of smaller particles to fresher sources was reported by Gu et al. (2011), who reported a maximum number size distribution from fresh stationary combustion, peaking around 100 nm within the city of Augsburg, while Cusack et al. (2013) found the highest factor loading for particles between 100 and 300 nm for the factor attributed to "industrial + traffic + biomass burning" at a rural site.

Heating season (HS) $PM_{2.5}$ correlations (Table S2) generally support similar influences as seen overall. Specifically, while sulphate (0.84) and ammonium (0.84) HS correlation coefficients were similar to the whole period, the nitrate correlation was much lower (0.42). This may have been a result of the spatial variation of sulphate and nitrate in Europe (there is a higher influence of sulphate in eastern Europe and nitrate in western Europe; Bessagnet et al., 2004) in combination with meteorology that usually decreases aerosol concentration with westerly air masses and increases with easterly air masses (see below).

A similar influence of carbonaceous aerosol on $PM_{2.5}$ in HS to the overall one was supported by the similar correlation of $PM_{2.5}$ with OC (0.86) and EC (0.70). Similar industrial and coal combustion influence was supported by the correlation with Zn (0.90) and Pb (0.72) and the influence of biomass burning by correlation with K (0.86).

Despite the large similarity of the HS and whole period in correlation of $PM_{2.5}$ with chemical species, the correlation of $PM_{2.5}$ with particle number size fraction were larger (N300–800: 0.98) in HS, and also very high for smaller particles (N150–300: (0.92), N80–150: (0.83)). The last two high correlations suggested a higher influence of local sources during HS (Venkataramant and Friedlander, 1994; Reid et al., 1998) as small particle sizes in this case indicate fresher aerosol probably due to residential heating in nearby villages.

The HS correlation coefficient of sulphate and ammonium was 0.93. High correlations with Zn (0.75) and Pb (0.73) suggest a coal combustion and industrial source; however, the sources were not local, as correlation with N300–800 was 0.85, N150–300 was 0.68, and N80–150 was only 0.52. This is in agreement with a slow SO_2/SO_4^{2-} transformation, which did not allow for rapid sulphate formation from nearby SO_2 sources or liquid phase formation of sulphates (Hering and Friedlander, 1982)

Although HS carbonaceous aerosol have the same sources for the whole period (OC correlation coefficients: EC (0.75), Zn (0.87), K (0.83), LVG (0.67); EC: K (0.72), Zn (0.73), LVG (0.65)), an additional, probably traffic-based, source appeared. This is evidenced by the correlation of OC and EC with Fe (0.71 resp. 0.66). More importantly, local sources exhibited higher influences, which is reflected in the high correlations of OC with N150–300 (0.84) and N80–150 (0.81). These correlations were almost the same or even higher than for N300–800 (0.82). This effect was even more visible for EC (N80–150 (0.77) and N150–300 (0.76), as the correlation coefficient with N300–800 was only 0.64.

The iron was attributed to traffic due to its correlation with Zn (0.70), Cu(0.65), Pb (0.63), and, especially, N80–150 (0.70) and N150–300 (0.70) (Gu et al., 2011; Beddows et al., 2015) while it only had a coefficient of 0.60 for N300–800. This is in contrast with Zn and Pb correlations with N300–800, which exhibited maximum correlations (0.88 and 0.72).

An interesting correlation was found between Na and the smallest particles (N10–25 (0.63) and N25–50 (0.64)), which probably resulted from a dilution effect (enabling a longer lifetime and faster transport of the smallest particles) resulting from strong winds from westerly directions that allowed for efficient transport of sea salt or resuspended road salt to the site. The cleaning of the atmosphere might also facilitate conditions for new particle formation events through decreasing condensational sink. This is further supported by the significant anti-correlations between Na and $PM_{2.5}$ (−0.46) and N300–800 (−0.52).

Non-heating season (NHS) (Table S3) sources were significantly different from those found for the whole period, and, in some cases, the HS. Conversely, the industrial sources were the same for the NHS, HS, and whole period; $PM_{2.5}$ correlation with NH_4^+ (0.93), SO_4^{2-} (0.94), Pb (0.83), and Zn (0.76) were the most important. $PM_{2.5}$ regional or long-range transport and cloud processed origins were confirmed by the correlation with N300–800 (0.85) (Hering and Friedlander, 1982; John et al., 1990). A much smaller correlation was found for N150–300 (0.54). Some influence of nitrates on $PM_{2.5}$ is seen from their correlation coefficient of 0.72. Only low correlations with OC and EC were found, suggesting different sources of $PM_{2.5}$ mass concentration build-up and carbonaceous aerosol during the NHS.

Sulphate correlations confirmed the aged industrial and coal combustion origins (correlation coefficients: NH4+ (0.95), Pb (0.89), Zn (0.71), and N300–800 (0.87)). The nitrate correlation suggested the influence of aged biomass combustion and/or meteorological conditions that were favourable for both pollutants (cold weather stabilizes ammonium nitrate and may be the cause of shorter periods of residential heating, when wood is often used instead of coal (LVG (0.75), NH4+ (0.79), Zn (0.71), and N300–800 (0.71)). The same may cause a strong correlation with Cl^- (0.90), as ammonium chloride dissociation/evaporation behaviour is similar to ammonium nitrate.

Carbonaceous aerosol, and especially OC, exhibited much lower correlations with other species, the highest being for LVG (0.69) and EC (0.67). This, together with EC correlations with K (0.77) and LVG (0.65), suggests the influence of biomass burning during the NHS, which was probably connected with agricultural and forest works burning. Another possible explanation may have been the presence of an industrial boiler (32 MW, http://portal.chmi.cz/files/portal/docs/uoco/web_generator/plants/688770041_CZ.html), located 10 km SW of the Košetice site, which used wooden pellets as a fuel source. A maximum correlation coefficient of OC with particle number size fraction was found for N80–150 (0.58), which supports the influence of fresh aerosol. This may also support the influence of biogenic SOA formation, which is not correlated with any other species. The strong correlation between K and EC may also be due to emissions from the wooden pellet boiler, as such an appliance was found to emit higher amounts of EC and K, and less OC (Wierzbicka et al., 2005).

Besides the species that account for most of the $PM_{2.5}$ mass, there were a group of crustal elements probably representing long-range transported or resuspended dust that were mainly mutually correlated during NHS when, for example, Al correlates with Ca (0.73), Fe (0.69), Si (0.72), and Ti (0.71).

Unusually high NHS correlations were found between Mn and K ($r = 0.81$), which is difficult to explain. A NHS source of K is connected with Mn, but also with EC (K/EC 0.77, Mn/EC 0.49). Significant correlations between Mn and crustal elements were also found. Common sources of Mn, K, and EC may be the industrial boiler, but also traffic. Both K and Mn organic compounds are used as gasoline additives for replacing lead or sold as octane booster additives (e.g. http://images.toolbank.com/downloads/cossh/1239.pdf, http://lucasoil.com/pdf/SDS_Octane-Booster.pdf). Additionally, the glass industry present within the broader area around the site, might have been a common source of K and Mn.

3.5. Air masses

The average and median concentrations of the $PM_{2.5}$ and chemical components were calculated for each category of air mass. The ratios of individual species average mass concentrations for each AMBT to overall average were evaluated and compared for each AMBT category (Fig. 4). A similar exercise was done for relative share of individual species in $PM_{2.5}$ mass (Fig. 5). The differences between the ratios for each

AMBT will be discussed further, while the ratios of medians will be mentioned only when their distributions among AMBT categories differ substantially.

Each AMBT category exhibited some chemical species with a corresponding maximum ratio to the species overall average concentration, but the differences between AMBT categories were generally lower in ratios of their relative concentrations in $PM_{2.5}$ than between the ratios of species' absolute concentrations. Fig. 4 shows total $PM_{2.5}$ had the highest concentrations in Econt air masses (the only category with above annual average concentrations), and was followed by SW, Wcont, and, the lowest concentration, NW air masses. Maximum ratios to a species' overall average concentrations were also found in the Econt air masses for sulphates, nitrates, ammonium, zinc, and lead. These results show very similar tendencies (even quantitatively) as that described for inorganic ions and EC in Melpitz (Spindler et al., 2004, 2010), suggesting significant transport of pollution from Eastern Europe. Vodička et al. (2015) also suggested the influence of long-range transport through easterly winds for the Košetice site based on OC/EC data and comparison with a Prague site. However, the influence of meteorological conditions in Central Europe may have also influenced the results, as will be discussed below.

The SW air masses were probably influenced by Saharan dust events. Both absolute average concentrations and relative shares (Fig. 5) of Al, Si, Ti, Ca, and Fe for this air mass were almost twice as high as the study's overall average.

Apart from these elements, there were only a few other species with maxima in SW air masses. As, LVG, K, and EC had maxima in SW air masses, both in absolute and relative terms, while OC displayed only a relative maxima in this air mass, which was only slightly higher than the absolute maximum in E air masses. This suggests both coal and biomass combustion sources influenced SW air masses more than the other air masses. The higher average and median NO/NO_2 ratio and NO_x concentration in SW air masses suggest the influence of nearby combustion sources, due to relatively quick oxidation of NO to NO_2 during its atmospheric transport (Harrison et al., 1998; Minoura and Ito, 2010). The village of Kramolin and/or the industrial boiler may have been at least partially responsible for maxima of these species in SW air masses.

Copper is the only analysed species that exhibited both absolute and relative concentration maxima in the Wcont air masses. This indicates the influence of brake debris or an industrial source, but no concrete reason can be determined. Median Wcont concentrations did not show an increase, and a very high standard deviation of the mean Cu concentrations suggests the influence of a few outliers of unknown origin.

NW air masses contained minimum concentrations for most species; however, sea salt species were elevated. Na was substantially higher, both in absolute (Fig. 4) and relative terms (Fig. 5), while the Mg absolute concentration was slightly higher and the relative concentration was much higher. Cl was only higher in the relative scale, which was probably due to the transformation of chlorides to nitrates during transport to Central Europe (Pakkanen, 1996; Schwarz et al., 2012). Nitrate exhibited a relative maximum concentration in NW air masses, which was probably due to lower sulphate levels and, on average, lower temperatures (5.2 °C NW, 8.3 °C average). The small influence of sea salt transformed to nitrates cannot be excluded.

During the evaluation of this relatively small sample set, we took into account that the data subsets were influenced by local weather and/or seasonal effects that were not evenly distributed among the AMBT categories.

The most important meteorological parameter affecting aerosol levels was temperature, as it often directly impacted domestic heating related species (mainly LVG, K, Zn, Pb, and As, whose mean concentrations were at least twice as high for $T < 0$ °C than during the warmest days, which had an average of $T > 15$ °C; Fig. S2). During this study, the average temperatures were similar for all air masses (Econt 8.6 °C, SW 9.3 °C, Wcont 10.6 °C), except NW AMBT (5.2 °C), which also had the lowest median temperature. Among all AMBT categories, both the average and median $PM_{2.5}$ concentrations were the lowest for the NW. Average and median wind speeds were also the highest (NW average 2.1 m/s) for this AMBT, which contribute to PM2.5 concentration reduction in contrast with wind speeds for the other air masses (Econt 1.5 m/s, SW 1.5 m/s, Wcont 1.6 m/s).

The highest concentrations of $PM_{2.5}$, SO_4^{2-}, NH_4^+, Zn, and Pb were recorded during Econt AMBT. Average temperatures, wind speed, and RH under this air mass were similar to the other two air mass categories, while median temperatures were the second highest. Thus, higher concentrations in this category cannot be directly related to meteorological conditions, but, rather, must be associated with the air mass origin. In this case, elevated pollution associated with these air masses were probably a result of emissions in the industrial region of Salesia, located in the NE of the Czech Republic, southern Poland, and the large urban agglomerations of Vienna and Budapest (around 5 million inhabitants combined). SO_2 sources in southeastern Europe (Pouliot et al. 2012) may have also increased levels of pollutants from this direction.

The influence of wind speed on $PM_{2.5}$ levels is largely reflected in local, or relatively local, emissions and proximity to aerosol sources. Under low wind speeds (<1 m s^{-1}), levels increased for LVG, K, Mn, and EC, indicating that these components have a local source, most likely biomass burning and traffic.

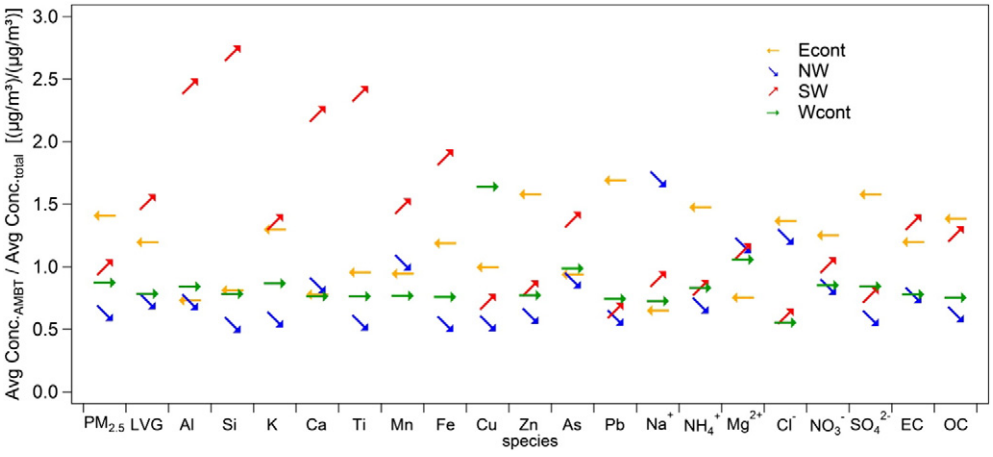

Fig. 4. Ratios of each AMBT average concentrations to the overall average concentration of individual species.

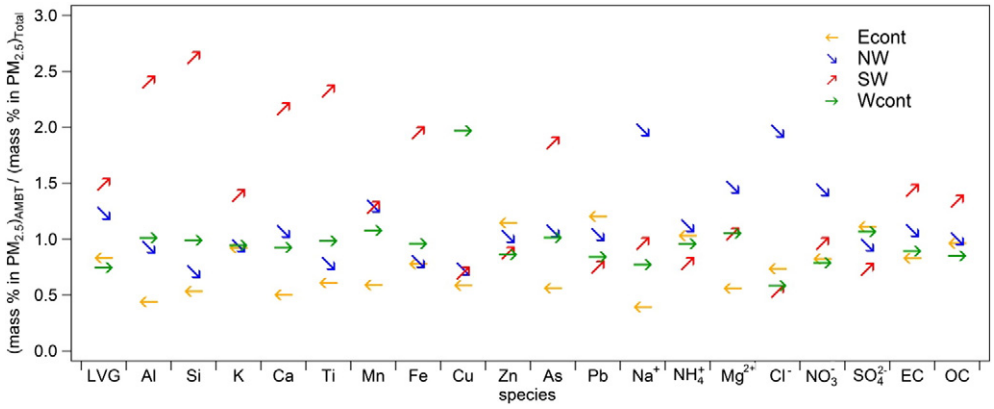

Fig. 5. Ratios of each AMBT average percentage to the overall average percentage of individual species in $PM_{2.5}$ mass.

4. Conclusions

A comprehensive study of $PM_{2.5}$ chemical composition at the Central European rural background site, Košetice, is presented and discussed, and the data are compared with recently published data from other rural background sites in Europe. The results showed similar levels of $PM_{2.5}$ to other Central European rural background sites.

Chemical analysis showed that carbonaceous aerosols form about half of $PM_{2.5}$ mass. The remaining half is mostly composed of secondary inorganic aerosol, with a higher share of sulphates relative to nitrates. A typical Central European seasonal variability of $PM_{2.5}$, with winter maxima and summer minima, was found.

The seasonal variability of LVG, potassium, zinc, and lead, with high winter maxima, revealed the strong influence of residential heating via both wood and coal combustion. Similar seasonal behaviour of OC, with a slightly higher share in winter, suggested the higher influence of combustion aerosol in winter than the influence of SOA formation in summer. A less pronounced seasonality of EC than OC, despite residential heating combustion emissions in winter, supports the similar influence of traffic throughout the year.

Thermodynamically driven behaviour, with maximum in winter and very low minima in summer, was common for nitrates and chlorides, supporting the major influence of ammonium salts on their concentrations throughout the year. Although a small amount of sea salt was occasionally present, most of the chlorides were replaced by nitrates during transport to the site. Crustal elements were the only species with maxima during summer.

Mass closure showed that, on average, 45% of $PM_{2.5}$ was formed of OM, of which one-third (14% of $PM_{2.5}$) was, based on LVG analysis, formed by OM_{BB}.

The seasonal share of OM_{BB} in $PM_{2.5}$ was 4% in summer and 19% in winter, totalling almost 40% of OM at this site. This high biomass combustion influence was also seen from the analysis of the Spearman correlation coefficients matrix with $PM_{2.5}$, individual species, and particle number concentrations in several size fractions.

The analysis showed the prevailing influence of aged aerosol, especially during the NHS, when aged industrial and coal combustion sources probably dominated $PM_{2.5}$ aerosol. SOA formation could be inferred only indirectly from our results, while some biomass combustion influence was seen clearly.

While aged industrial and coal combustion sources remained mainly connected with the largest particle size fraction measured by SMPS during the HS, biomass and wood combustion tracers exhibited a closer connection with smaller particles, showing the presence of fresher aerosol. This influence was also reflected in $PM_{2.5}$ correlations with particle size fractions due to the high influence of biomass burning during the HS.

Air mass back trajectory analysis revealed that Easterly continental air masses are more loaded with higher levels of $PM_{2.5}$ than westerly air masses, including those that remained above the continent for 96 h before arriving to the site. The cleanest air mass comes from fast moving NW air masses. A dilution effect connected with these clean air masses was observed via the correlation of the smallest particle size fractions with Na.

These different correlations of individual species with different size fractions suggests externally mixed particles at least during the heating season, even at this rural background site. They also show that there is some influence of local sources and that, consequently, care must be applied if the data are used for long-range transport assessment.

More data are needed to enable full PMF source apportionment analysis of $PM_{2.5}$ at this site.

Acknowledgements

This work was supported by the Czech Science Foundation grant No. P209/11/1342, the European Union Seventh Framework Programme (FP7/2007-2013) under the ACTRIS project with grant agreement No. 262254, and from the EU FP6 project “European Supersites for Atmospheric Aerosol Research” (EUSAAR). The PIXE analysis was done under the CANAM (Center of Accelerators and Nuclear Analytical Methods LM2011019) infrastructure at NPI ASCR v.v.i. The authors also thank Kayleigh Kavanagh for the language revision.

Appendix A. Supplementary data

Supplementary data to this article can be found online at http://dx.doi.org/10.1016/j.atmosres.2016.02.017.

References

Beddows, D.C.S., Harrison, R.M., Green, D.C., Fuller, G.W., 2015. Receptor modelling of both particle composition and size distribution from a background site in London, UK. Atmos. Chem. Phys. 15 (17), 10107–10125.

Berglund, J., Fronaeus, S., Elding, L.I., 1993. Kinetics and mechanism for manganese-catalyzed oxidation of sulphur(IV) by oxygen in aqueous-solution. Inorg. Chem. 32 (21), 4527–4538.

Bessagnet, B., Hodzic, A., Vautard, R., Beekmann, M., Cheinet, S., Honoré, C., Liousse, C., Rouila, L., 2004. Aerosol modeling with CHIMERE—preliminary evaluation at the continental scale. Atmos. Environ. 38 (18), 2803–2817.

Birch, M.E., Cary, R.A., 1996. Elemental carbon-based method for monitoring occupational exposures to particulate diesel exhaust. Aerosol Sci. Technol. 25, 221–241.

Birmili, W., Schepanski, K., Ansmann, A., et al., 2008. A case of extreme particulate matter concentrations over Central Europe caused by dust emitted over the southern Ukraine. Atmos. Chem. Phys. 8 (4), 997–1016.

Borbely-Kiss, I., Koltay, E., Szabo, G.Y., et al., 1999. Composition and sources of urban and rural atmospheric aerosol in eastern Hungary. J. Aerosol Sci. 30 (3), 369–391.

Bressi, M., Sciare, J., Ghersi, V., Bonnaire, N., Nicolas, J.B., Petit, J.-E., Moukhtar, S., Rosso, A., Mihalopoulos, N., Féron, A., 2013. A one-year comprehensive chemical characterisation of fine aerosol (PM2.5) at urban, suburban and rural background sites in the region of Paris (France). Atmos. Chem. Phys. 13 (15), 7825–7844.

Caseiro, A., Bauer, H., Schmidl, C., Pio, C.A., Puxbaum, H., 2009. Wood burning impact on PM10 in three Austrian regions. Atmos. Environ. 43, 2186–2195.
Cavalli, F., Viana, M., Yttri, K.E., Genberg, J., Putaud, J.-P., 2010. Towards a standardized thermal-optical protocol for measuring atmospheric organic and elemental carbon: The EUSAAR Protocol. Atmos. Meas. Tech. 3, 79–89.
Chow, J.C., Watson, J.G., Crow, D., Lowenthal, D.H., Merrifield, T., 2001. Comparison of IMPROVE and NIOSH carbon measurement. Aerosol Sci. Technol. 34, 23–34.
Cusack, M., Perez, N., Pey, J., Alastuey, A., Querol, X., 2013. Source apportionment of fine PM and sub-micron particle number concentrations at a regional background site in the western Mediterranean: a 2.5 year study. Atmos. Chem. Phys. 13 (10), 5173–5187.
Draxler, R.R., Rolph, G.D., 2013. HYSPLIT (HYbrid Single-Particle Lagrangian Integrated Trajectory) Model access via NOAA ARL READY Website (http://www.arl.noaa.gov/HYSPLIT.php). NOAA Air Resources Laboratory, College Park, MD.
Duvall, R.M., Norris, G.A., Dailey, L.A., Burke, J.M., McGee, J.K., Gilmour, M.I., et al., 2008. Source apportionment of particulate matter in the U.S. and associations with lung inflammatory markers. Inhal. Toxicol. 20 (7), 671–683.
Elsasser, M., Busch, C., Orasche, J., Schön, C., Hartmann, H., Schnelle-Kreis, J., Zimmermann, R., 2013. Dynamic changes of the aerosol composition and concentration during different burning phases of wood combustion. Energy Fuel 27 (8), 4959–4968.
El-Zanan, H.S., Lowenthal, D.H., Zielinska, B., Chow, J.C., Kumar, N., 2005. Determination of the organic aerosol mass to organic carbon ratio in IMPROVE samples. Chemosphere 60 (4), 485–496.
Fabbri, D., Torri, C., Simoneit, B.R., Marynowski, L., Rushdi, A.I., Fabiańska, M.J., 2009. Levoglucosan and other cellulose and lignin markers in emissions from burning of Miocene lignites. Atmos. Environ. 43 (14), 2286–2295.
Fine, P.M., Cass, G.R., Simoneit, B.R., 2001. Chemical characterization of fine particle emissions from fireplace combustion of woods grown in the northeastern United States. Environ. Sci. Technol. 35 (13), 2665–2675.
Gelencsér, A., May, B., Simpson, D., Sánchez-Ochoa, A., Kasper-Giebl, A., Puxbaum, H., Caseiro, A., Pio, C., Legrand, M., 2007. Source apportionment of PM2. 5 organic aerosol over Europe: primary/secondary, natural/anthropogenic, and fossil/biogenic origin. J. Geophys. Res. Atmos. 112 (D23), 1984–2012.
Gilardoni, S., Vignati, E., Cavalli, F., Putaud, J.P., Larsen, B.R., Karl, M., Stenström, K., Genberg, J., Henne, S., Dentener, F., 2011. Better constraints on sources of carbonaceous aerosols using a combined C-14–macro tracer analysis in a European rural background site. Atmos. Chem. Phys. 11 (12), 5685–5700.
Gu, J., Pitz, M., Schnelle-Kreis, J., Diemer, J., Reller, A., Zimmermann, R., Soentgen, J., Stoelzel, M., Wichmann, H.-R., Peters, A., Cyrys, J., 2011. Source apportionment of ambient particles: comparison of positive matrix factorization analysis applied to particle size distribution and chemical composition data. Atmos. Environ. 45 (10), 1849–1857.
Harrison, R.M., Sturges, W.T., Kitto, A., Li, Y., 1990. Kinetics of evaporation of ammonium chloride and ammonium nitrate aerosols. Atmos. Environ. Part A 24 (7), 1883–1888.
Harrison, R.M., Shi, J.P., Grenfell, J.L., 1998. Novel nighttime free radical chemistry in severe nitrogen dioxide pollution episodes. Atmos. Environ. 32 (16), 2769–2774.
Hartman, M., Trnka, O., Svoboda, K., Vesely, V., 2003. Thermal dissociation and H_2S reactivity of Czech limestones. Chem. Pap. - Slovak Acad. Sci. 57 (5), 309–316.
Havránek, V., Hnatowicz, V., Kvítek, J., Obrusník, I., 1994. PIXE-INP computer code for analyses of thin and thick samples. Nucl. Inst. Methods B85, 637–641.
Havránek, V., Voseček, V., Novotný, J., 2004. New Experimental Target Chamber for imultaneous PIXE, PIGE, RBS and PESA Analysis. Proceedings of 10th International Conference on Particle Induced X-ray Emission and its Analytical Applications, PIXE 2004, Portorož, Slovenia, pp. 822.1–822.3 (ISBN 961-6303-62-67).
Hering, S.V., Friedlander, S.K., 1982. Origins of aerosol sulfur size distributions in the Los Angeles basin. Atmos. Environ. 16, 2647–2656.
Hladil, J., Strnad, L., Šálek, M., Jankovská, V., Šimandl, P., Schwarz, J., Smolík, J., Lisá, L., Koptíková, L., Rohovec, J., Böhmová, V., Langrová, A., 2008. An anomalous atmospheric dust deposition event over Central Europe, 24 March 2007, and fingerprinting of the SE Ukrainian source. Bull. Geosci. 83 (2), 175–206.
Horváth, L., Sutton, M.A., 1998. Long-term record of ammonia and ammonium concentrations at K-Puszta, Hungary. Atmos. Environ. 32 (3), 339–344.
Horvath, H., Kasaharat, M., Pesava, P., 1996. The size distribution and composition of the atmospheric aerosol at a rural and nearby urban location. J. Aerosol Sci. 27 (3), 417–435.
http://images.toolbank.com/downloads/cossh/1239.pdf
http://lucasoil.com/pdf/SDS_Octane-Booster.pdf
http://portal.chmi.cz/files/portal/docs/uoco/web_generator/plants/688770041_CZ.html
Hueglin, C., Gehrig, R., Baltensperger, U., Gysel, M., Monn, C., Vonmont, H., 2005. Chemical characterisation of PM2.5, PM10 and coarse particles at urban, near-city and rural sites in Switzerland. Atmos. Environ. 39, 637–651.
Jedynska, A., Hoek, G., Wang, M., Eeftens, M., Cyrys, J., Beelen, R., Cirache, M., De Nazelle, A., Keuken, M., Visschedijk, A., Nystad, W., Akhlaghi, H.M., Meliefste, K., Nieuwenhuijsene, M., de Hoogh, K., Brunekreef, B., Kooter, I.M., 2015. Spatial variations of levoglucosan in four European study areas. Sci. Total Environ. 505, 1072–1081.
John, W., Wall, S.M., Ondo, J.L., Winklmayr, W., 1990. Modes in the size distributions of atmospheric inorganic aerosol. Atmos. Environ. 24A, 2349–2359.
Kopáček, J., Prochazkova, L., Hejzlar, J., Blažka, P., 1997. Trends and seasonal patterns of bulk deposition of nutrients in the Czech Republic. Atmos. Environ. 31 (6), 797–808.
Lai, C., Liu, Y., Ma, J., Ma, Q., He, H., 2014. Degradation kinetics of levoglucosan initiated by hydroxyl radical under different environmental conditions. Atmos. Environ. 91, 32–39.
Limbeck, A., Handler, M., Puls, C., Zbiral, J., Bauer, H., Puxbaum, H., 2009. Impact of mineral components and selected trace metals on ambient PM10 concentrations. Atmos. Environ. 43 (3), 530–538.
Lough, G.C., Schauer, J.J., Park, J.S., et al., 2005. Emissions of metals associated with motor vehicle roadways. Environ. Sci. Technol. 39 (3), 826–836.
Machálek, P., Machart, J., 2003. Emisní balance vytápění bytů malými zdroji od roku 2001. (The emission balance of residential heating using small heat sources from the year 2001, in Czech). Český hydrometeorologický ústav, oddělení emisí a zdrojů, pracoviště Milevsko, Milevsko.
Maenhaut, W., Raes, N., Chi, X., Cafmeyer, J., Wang, W., Salma, I., 2005. Chemical composition and mass closure for fine and coarse aerosols at a kerbside in Budapest, Hungary, in spring 2002. X-Ray Spectrom. 34, 290.
Maenhaut, W., Raes, N., Chi, X., Cafmeyer, J., Wang, W., 2008. Chemical composition and mass closure for PM2.5 and PM10 aerosols at K-Puszta, Hungary, in summer 2006. X-Ray Spectrom. 37, 193–197.
Minoura, H., Ito, A., 2010. Observation of the primary NO_2 and NO oxidation near the trunk road in Tokyo. Atmos. Environ. 44 (1), 23–29.
Pacyna, J.M., Pacyna, E.G., 2001. An assessment of global and regional emissions of trace metals to the atmosphere from anthropogenic sources worldwide. Environ. Rev. 9 (4), 269–298.
Pacyna, E.G., et al., 2007. Current and future emissions of selected heavy metals to the atmosphere from anthropogenic sources in Europe. Atmos. Environ. 41 (38), 8557–8566.
Pakkanen, T.A., 1996. Study of formation of coarse particle nitrate aerosol. Atmos. Environ. 30 (14), 2475–2482.
Pio, C.A., Legrand, M., Oliveira, T., Afonso, J., Santos, C., Caseiro, A., Fialho, P., Barata, F., Puxbaum, H., Sanchez-Ochoa, A., Kasper-Giebl, A., Gelencsér, A., Preunker, S., Schock, M., 2007. Climatology of aerosol composition (organic versus inorganic) at nonurban sites on a west-east transect across Europe. J. Geophys. Res. Atmos. 112 (D23), 1984–2012.
Poulain, L., Spindler, G., Birmili, W., Plass-Dülmer, C., Wiedensohler, A., Herrmann, H., 2011. Seasonal and diurnal variations of particulate nitrate and organic matter at the IfT research station Melpitz. Atmos. Chem. Phys. 11 (24), 12579–12599.
Pouliot, G., Pierce, T., van der Gon, H.D., Shaap, M., Moran, M., Nopmoncol, U., 2012. Comparing emission inventories and model-ready emission datasets between Europe and North America for the AQMEII project. Atmos. Environ. 53 (SI), 4–14.
Putaud, J.-P., Raes, F., Van Dingenen, R., Brueggemann, E., Facchini, M.C., Decesari, S., Fuzzi, S., Gehrig, R., Hueglin, C., Laj, P., Lorbeer, G., Maenhaut, W., Mihalopoulos, N., Mueller, K., Querol, X., Rodriguez, S., Wiedensohler, A., 2004. A European aerosol phenomenology—2: Chemical characteristics of particulate matter at kerbside, urban, rural and background sites in Europe. Atmos. Environ. 38, 2579–2595.
Putaud, J.-P., Van Dingenen, R., Alastuey, A., Bauer, H., Birmili, W., Cyrys, J., Flentje, H., Fuzzi, S., Gehrig, R., Hansson, H.C., Harrison, R.M., Herrmann, H., Hitzenberger, R., Hüglin, C., Jones, A.M., Kasper-Giebl, A., Kiss, G., Kousa, A., Kuhlbusch, T.A.J., Löschau, G., Maenhaut, W., Molnar, A., Moreno, T., Pekkanen, J., Perrino, C., Pitz, M., Puxbaum, H., Querol, X., Rodriguez, S., Salma, I., Schwarz, J., Smolik, J., Schneider, J., Spindler, G., ten Brink, H., Tursic, J., Viana, M., Wiedensohler, A., Raes, F.A., 2010. European aerosol phenomenology—3: Physical and chemical characteristics of particulate matter from 60 rural, urban, and kerbside sites across Europe. Atmos. Environ. 44 (10), 1308–1320.
Puxbaum, H., Gomiscek, B., Kalina, M., Bauer, H., Salam, A., Stopper, S., Preining, O., Hauck, H., 2004. A dual site study of PM2.5 and PM10 aerosol chemistry in the larger region of Vienna, Austria. Atmos. Environ. 38, 3949–3958.
Puxbaum, H., Caseiro, A., Sánchez-Ochoa, A., Kasper-Giebl, A., Claeys, M., Gelencsér, A., Preunkert, S., Legrand, M., Pio, C., 2007. Levoglucosan levels at background sites in Europe for assessing the impact of biomass combustion on the European aerosol background. J. Geophys. Res. Atmos. 112 (D23), 1984–2012.
Reid, J.S., Hobbs, P.V., Ferek, R., Blake, D.R., Vanderlei Martins, J., Dunlap, M.R., Liousse, C., 1998. Physical, chemical, and optical properties of regional hazes dominated by smoke in Brazil. J. Geophys. Res. 103 (D24), 32,059–32,080.
Rogula-Kozłowska, W., Klejnowski, K., Rogula-Kopiec, P., Ośródka, L., Krajny, E., Błaszczak, B., Mathews, B., 2014. Spatial and seasonal variability of the mass concentration and chemical composition of PM2. 5 in Poland. Air Qual. Atmos. Health 7, 41.
Rolph, G.D., 2013. Real-time Environmental Applications and Display sYstem (READY) Website (http://www.ready.noaa.gov). NOAA Air Resources Laboratory, College Park, MD.
Salameh, D., Detournay, A., Pey, J., Pérez, N., Liguori, F., Saraga, D., Bove, M.C., Brotto, P., Cassola, F., Massabò, D., Latella, A., Pillon, S., Formenton, G., Patti, S., Armengaudi, A., Piga, D., Jaffrezo, J.L., Bartzis, J., Tolis, E., Prati, P., Querol, X., Wortham, H., Marchand, N., 2015. PM2.5 chemical composition in five European Mediterranean cities: a 1-year study. Atmos. Res. 155, 102–117.
Schauer, J.J., Rogge, W.F., Hildemann, L.M., Mazurek, M.A., Cass, G.R., Simoneit, B.R.T., 1996. Source apportionment of airborne particulate matter using organic compounds as tracers. Atmos. Environ. 30, 3837–3855.
Schmidl, C., Luisser, M., Padouvas, E., Lasselsberger, L., Rzaca, M., Ramirez-Santa Cruz, C., Handler, M., Penga, G., Bauer, H., Puxbaum, H., 2011. Particulate and gaseous emissions from manually and automatically fired small scale combustion systems. Atmos. Res. 45 (39), 7443–7454.
Schwarz, J., Chi, X., Maenhaut, W., Civiš, M., Hovorka, J., Smolík, J., 2008. Elemental and organic carbon in atmospheric aerosols at downtown and suburban sites in Prague. Atmos. Res. 90, 287–302.
Schwarz, J., Stefancova, L., Maenhaut, W., Smolik, J., Zdimal, V., 2012. Mass and chemically speciated size distribution of Prague aerosol using an aerosol dryer—the influence of air mass origin. Sci. Total Environ. 437, 348–362.
Schwikowski, M., Seibert, P., Baltensperger, U., Gaggeler, H.W., 1995. A study of an outstanding Saharan dust event at the high-alpine site Jungfraujoch, Switzerland. Atmos. Environ. 29 (15), 1829–1842.

Seinfeld, J.H., Pandis, S.N., 1998. Atmospheric Chemistry and Physics. John Wiley & Sons, New York.
Siegismund, F., Schrum, C., 2001. Decadal changes in the wind forcing over the North Sea. Clim. Res. 18, 39–45.
Simoneit, B.R., Schauer, J.J., Nolte, C.G., Oros, D.R., Elias, V.O., Fraser, M.P., Rogge, W.F., Cass, G.R., 1999. Levoglucosan, a tracer for cellulose in biomass burning and atmospheric particles. Atmos. Environ. 33 (2), 173–182.
Sippula, O., Hokkinen, J., Puustinen, H., Yli-Pirila, P., Jokiniemi, J., 2009. Particle emissions from small wood-fired district heating units. Energy Fuel 23, 2974–2982.
Spindler, G., Müller, K., Brüggemann, E., Gnauk, T., Herrmann, H., 2004. Long-term size-segregated characterization of PM10, PM2. 5, and PM1 at the IfT research station Melpitz downwind of Leipzig (Germany) using high and low-volume filter samplers. Atmos. Environ. 38 (31), 5333–5347.
Spindler, G., Brüggemann, E., Gnauk, T., Grüner, A., Müller, K., Herrmann, H., 2010. A four-year size-segregated characterization study of particles PM10, PM2. 5 and PM1 depending on air mass origin at Melpitz. Atmos. Environ. 44 (2), 164–173.
Spindler, G., Grüner, A., Müller, K., Schlimper, S., Herrmann, H., 2013. Long-term size-segregated particle (PM10,PM2.5, PM1) characterization study at Melpitz—influence of air mass inflow, weather conditions and season. J. Atmos. Chem. 70, 165–195.
Swietlicki, E., Krejci, R., 1996. Source characterization of the Central European atmospheric aerosol using multivariate statistical methods. Nucl. Inst. Methods Phys. Res. B 109/110, 519–525.
Szidat, S., Ruff, M., Perron, N., Wacker, L., Synal, H.A., Hallquist, M., Shannigrahi, A.S., Yttri, K.E., Dye, C., Simpson, D., 2009. Fossil and non-fossil sources of organic carbon (OC) and elemental carbon (EC) in Göteborg, Sweden. Atmos. Chem. Phys. 9 (5), 1521–1535.
Turpin, B.J., Lim, H.J., 2001. Species contributions to PM2.5 mass concentrations: revisiting common assumptions for estimating organic mass. Aerosol Sci. Technol. 35, 602–610.
Uher, G., Schebeske, G., Barlow, R.G., Cummings, D.G., Mantoura, R.F.C., Rapsomanikis, S.R., Andreae, M.O., 2000. Distribution and air–sea gas exchange of dimethyl sulphide at the European western continental margin. Mar. Chem. 69 (3-4), 277–300.
Venkataramant, C., Friedlander, S.K., 1994. Size distributions of polycyclic aromatic hydrocarbons and elemental carbon. 2. Ambient measurements and effects of atmospheric processes. Environ. Sci. Technol. 28, 563–572.
Vodička, P., Schwarz, J., Cusack, M., Ždímal, V., 2015. Detailed comparison of OC/EC aerosol at an urban and a rural Czech background site during summer and winter. Sci. Total Environ. 518–519, 424–433.
Watson, J.G., Chow, J.C., Houck, J.E., 2001. PM2.5 chemical source profiles for vehicle exhaust, vegetative burning, geological material, and coal burning in Northwestern Colorado during 1995. Chemosphere 43 (8), 1141–1151.
Wiedensohler, A., Birmili, W., Nowak, A., Sonntag, A., Weinhold, K., Merkel, M., Wehner, B., Tuch, T., Pfeifer, S., Fiebig, M., Fjäraa, A.M., Asmi, E., Sellegri, K., Depuy, R., Venzac, H., Villani, P., Laj, P., Aalto, P., Ogren, J.A., Swietlicki, E., Williams, P., Roldin, P., Quincey, P., Hüglin, C., Fierz-Schmidhauser, R., Gysel, M., Weingartner, E., Riccobono, F., Santos, S., Grüning, C., Faloon, K., Beddows, D., Harrison, R., Monahan, C., Jennings, S.G., O'Dowd, C.D., Marinoni, A., Horn, H.-G., Keck, L., Jiang, J., Scheckman, J., McMurry, P.H., Deng, Z., Zhao, C.S., Moerman, M., Henzing, B., de Leeuw, G., Löschau, G., Bastian, S., 2012. Mobility particle size spectrometers: harmonization of technical standards and data structure to facilitate high quality long-term observations of atmospheric particle number size distributions. Atmos. Meas. Tech. 5, 657–685.
Wierzbicka, A., Lillieblad, L., Pagels, J., Strand, M., Gudmundsson, A., Gharibi, A., Swietlicki, E., Sanati, M., Bohgard, M., 2005. Particle emissions from district heating units operating on three commonly used biofuels. Atmos. Environ. 39 (1), 139–150.
Zdráhal, Z., Oliveira, J., Vermeylen, R., Claeys, M., Maenhaut, W., 2002. Improved method for quantifying levoglucosan and related monosaccharides in atmospheric aerosols and application to samples from urban and tropical locations. Environ. Sci. Technol. 36, 747–753.
Zhang, X., McMurry, P.H., 1992. Evaporative losses of fine particulate nitrates during sampling. Atmos. Environ. Part A 26 (18), 3305–3312.
Zíková, N., Ždímal, V., 2013. Long-term measurement of aerosol number size distributions at rural background station Košetice. Aerosol Air Qual. Res. 13, 1464–1474.